ELSEVIER

International Journal of Solids and Structures 41 (2004) 5945–5965

INTERNATIONAL JOURNAL OF SOLIDS and STRUCTURES

www.elsevier.com/locate/ijsolstr

Numerical simulation of rock behaviour through a discrete model

Alessio Nardin *, Bernhard A. Schrefler

Department of Structural and Transportations Engineering, University of Padua, Via F. Marzolo 9, I-35131 Padova, Italy

Received 23 April 2004

Abstract

A common problem of excavation machinery based on mechanical actions is the unknown interaction of the cutting tools with various types of soils. Due to the involved non-linearities, the numerical analysis of such phenomena is very complex. To overcome these drawbacks some authors proposed to model the soil as a collection of spheres.

In this paper we apply a strategy for soil modelling which is based on discretization of the soil with rigid disks and suitable contact models. The basic idea is to concentrate at the contact level the real mechanical behaviour of the soil. The goal is achieved by extending the general concept of contact as an unilateral constraint condition, through a suitable constitutive law: the contact laws have been implemented in the node-to-segment contact formulation within the framework of the penalty method.

The aim of this work is to study the behaviour of some soils under different loading conditions, and to develop contact constitutive laws suitable for the discrete model. In order to carry out the proposed strategy a "macro" and a "micro" level are established, and macromechanical and micromechanical models are developed. In the micromechanical model the mutual contact interaction between two disks is studied, while the macromechanical model deals with the behaviour of a regular array of disks. The framework for the plastic behaviour of the contact element consists of a failure criterion; a one-dimensional, rate-independent elasto-plastic flow rule for normal and tangential force; two specific yield surfaces, and a hardening or softening law. In this paper we have focused our attention on the simulation of soils and rocks: a new constitutive contact law is developed and applied for the simulation of different soils with different testing conditions (such as uniaxial and shear tests).

Keywords: Elasto-plastic micromechanical model; Elasto-plastic macromechanical model; Soil behaviour; Contact mechanics; Granular media; Sensitivity analysis

* Corresponding author. Tel.: +39 049 8275619; fax: +39 049 8275604.
E-mail addresses: nardin@caronte.dic.unipd.it (A. Nardin), bas@caronte.dic.unipd.it (B. Schrefler).

0020-7863/$ - see front matter © 2004 Elsevier Ltd. All rights reserved.
doi:10.1016/j.ijsolstr.2004.05.071

1. Introduction

A common feature of many civil engineering and mining projects is that the earth surface has to be remodelled or removed for specific construction needs. Nowadays manpower is replaced by blasting technique and excavation machines like dredges, dozers, trenchers, roadheaders, etc. All these machines have their specific advantages and applications. An usual problem of excavation machinery based on mechanical actions is the unknown interaction of the cutting tools with various types of rock and more in general with geological settings. The problem is very important for the industry. In fact the interaction of the cutting tools with various soils determines a different wear and consequently different economical costs for the excavation. Due to the involved non-linearities, the numerical analysis of such phenomena is very complex. The classical continuum approach for modelling of soil presents several drawbacks, especially when large strains and crack propagation take place. To overcome the non-linear aspects some authors proposed to model the soil as a collection of spheres (Cundall and Strack, 1979; Emeriault and Cambou, 1996; Potyondy et al., 1996).

In this paper we apply a strategy for soil modelling based on discretization of the soil with rigid disks (plane strain) and suitable contact models. The idea is to concentrate at the contact level the real mechanical behaviour of the soil. The goal is achieved by extending the general concept of contact as a unilateral constraint condition, through a suitable constitutive law. For this purpose constitutive laws have been implemented in the node-to-segment contact formulation within the framework of the penalty method. In this case the penalty parameter is not a constant, but it is transformed into a non-linear function through the constitutive law itself (Zavarise et al., 1992). In such a way any tool penetration, crack propagation or change of shape of the soil will be transformed into a series of contact openings and/or slidings.

In our strategy the continuum is discretized as a collection of rigid disks suitably linked with special contact elements. Hence the displacement of a control volume (see Fig. 1) results from the overlapping of the disks. The equivalent mechanical answer is then governed by the contact law, which transforms the classical error of a penalty contact formulation into the required displacement field. With this respect it has to be remarked that

- the contact formulation deals with nodal forces and relative displacements;
- the contact force is the resultant of the contact stresses on the contact area associated with each contact node;
- a contact constitutive law is suitably tuned to get the equivalent global answer, still in terms of forces and displacements;
- from the above values a mean equivalent strain and stress field can be recovered for the control volume (see Fig. 1).

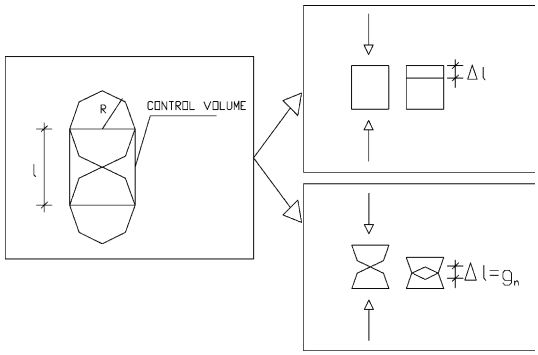

Fig. 1. Equivalent stress and strain definition for the micromechanical model.

In the following we refer to these last two quantities. An analogous equivalence can be defined also for the tensile behaviour, using a cohesive contact law.

The aim of this work is to study the behaviour of some soils under different loading conditions, and to develop contact constitutive laws suitable for the discrete model. In order to carry out the proposed strategy a "macro" and a "micro" level are established: in the micromechanical model the mutual contact interaction between two disks is studied. An elasto-plastic frictional contact law is developed to simulate the real behaviour of geomaterials (Nardin et al., 2003a). In the macromechanical model the behaviour of a random array of disks is described. Upscaling will be needed to link the micro- to the macromodel.

The following strategy has been proposed to obtain the "tracking" relationship:

- a behaviour of the micromechanical model similar to that of the real soil will first be obtained, where the values of the microparameters will be defined by a trial and error procedure;
- the values of these parameters will be calibrated through an upscaling law to reproduce with the macromechanical model the real behaviour of the soil.

The contact models are based on the classical concepts of elasticity and plasticity theories, with suitable modifications. The framework for the plastic behaviour consists of a failure criterion; a one-dimensional, rate-independent elasto-plastic flow rule for normal and tangential force; two specific yield surfaces, and a hardening or softening law (according to the real behaviour of the examined material).

In this paper we have focused our attention on the micromechanical model: a new constitutive contact law is developed and applied to the simulation of different soils and different tests (such as uniaxial and shear tests). Finally the behaviour of a regular and irregular array of disks will be studied. Numerical results show that by tuning appropriately the parameters, the behaviour of real soil can be simulated in a very effective way.

2. The Contact laws

In a previous paper (Nardin et al., 2003a) we have adapted some well-known failure criteria, such as Drucker-Prager, Burzynski and Tsai-Wu, to this contact framework. Successively a new constitutive law has been developed. This approach differs from the previous one because we started from the geometrical definition of the contact element (in the framework of the finite element theory) and developed a suitable constitutive law for normal and tangential contact. A multi-parameters failure criterion completes this procedure. This approach involves a greater number of parameters; however is more general than the previous one because it gives more freedom for matching experimentally observed behaviour. This is particularly important when using very complex tools for parameter identification (such as Artificial Neural Network (ANN) technique), because the constitutive model must be sufficiently rich such as to well cover the expected real behaviour to be modelled (Nardin et al., 2003b; Lefik and Schrefler, 2002).

A sensitivity analysis for this new model is carried out in this paper. Then the application of the model to different soils and the behaviour of a regular and irregular array of disks will be shown.

2.1. Micromechanical model

We represent the continuum as an assembly of cylindrical rigid discrete elements (disks). The reproduction of material properties is obtained through a suitable contact law between the disks. The contact law is

based on the classical concepts of elasto-plasticity theories, with suitable modifications. At contact level the elastic modulus, shear modulus and the Poisson ratio are here not linked through the classical relation, because the normal and tangential behaviour are treated separately. The normal and tangential elastic contact stiffnesses are supposed to remain constant. According to these assumptions the elastic part of the normal stress–strain relation is linear. The elasto-plastic relationships are established for both normal and tangential direction (Simo and Hughes, 1998) as

$$\sigma_i(F_i) = E_i \cdot (\varepsilon_i(g_i) - \varepsilon_i^{\mathrm{p}}(g_i^{\mathrm{p}})), \quad i = n, t \tag{1}$$

where σ_i is the normal or tangential stress, ε_i is the total strain, $\varepsilon_i^{\mathrm{p}}$ is the plastic component of the total strain, F_i is the contact force, g_i is the total relative displacement between two disks, g_i^{p} is the plastic component of the relative displacement, n, t are the normal and tangential directions; E_i are the parameters which characterize the elastic properties of the soil (see Fig. 2).

The yield function is defined for the normal stress–strain relation and for the tangential one. A general non-linear yield criterion has been formulated as follows:

$$f(\sigma_i, \alpha_i) = \mid \sigma_i \mid -[\sigma_Y + H(\alpha_i)]; \quad i = n, t \tag{2}$$

where $H(\alpha)$ is the expression of plastic strain and is written as function of the softening or hardening parameter, $\alpha : [0, T] \to \Re_+$, σ_Y is the limit of the elastic range. By changing these parameters we can define different shapes of the yield locus and simulate different soil behaviours.

The plastic strain increment, in normal and tangential direction, can be completely described for any admissible state of stress $\sigma_i \in E_\sigma$ by

$$\begin{aligned} &\dot{\varepsilon}_i^{\mathrm{p}} = \gamma_i \cdot sign(\sigma_i); \\ &E_\sigma = \{(\sigma_i, \alpha_i) \in \Re \times \Re_+ \mid f(\sigma_i, \alpha_i) \leqslant 0\} \quad i = n, t \end{aligned} \tag{3}$$

where $\dot{\varepsilon}^{\mathrm{p}} : [0, T] \to \Re$ is the time derivative of the plastic strain (normal or tangential), T is the time parameter, $\gamma \geqslant 0$ is the absolute value of the slip rate and its variation is calculated trough the consistency

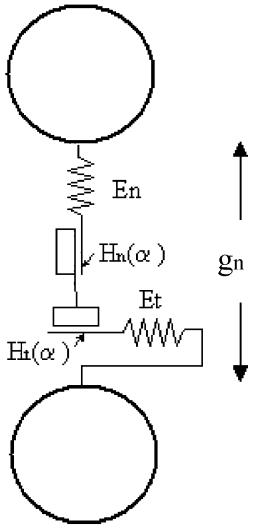

Fig. 2. Schematization of the contact law components in the micromechanical model.

parameter $\Delta\gamma$ and E_σ is the domain of the admissible stresses. The adopted evolution equations for α in the normal and in the tangential contact law are

$$\dot{\alpha}_n = |\dot{\varepsilon}_n^p|; \quad \dot{\alpha}_t = |\dot{\varepsilon}_t^p| \tag{4}$$

The value of the variable α_t and the shape of the tangential plastic function $H(\alpha_t)$ are independent from the respective normal values. The shape of the tangential yield surface depends directly on the applied failure criterion. In our approach the variability of the tangential stress due to the influence of the normal one is expressed by means of a two-dimensional failure criterion. This means that at each step the numerical value of the normal stress is fixed and a two-dimensional yield surface is used to establish the elastic range of the tangential stress, as shown in Fig. 3.

In the failure criterion the slip between two surfaces of a continuum is assumed to occurs when the shear stress, τ, on any plane at a point in the soil material reaches a critical value, which depends non-linearly upon the normal stress in the same plane.

In the strength criterion the shear strength of a rock-like material is made up of two parts varying with the normal applied stress: an elastic "cohesive" part and a frictional plastic part. The shear strength can be written as follows:

$$\tau = E_t(\sigma_n) \cdot (\varepsilon_t - \varepsilon_t^p) - (\tilde{n}(\sigma_n) + H(\alpha)) \tag{5}$$

where τ is the tangential critical stress; σ_n is the applied normal stress; ε_t and ε_t^p are respectively the total and the plastic tangential strain, H is the non-linear function of plasticity described in Eq. (2), and α is obtained from the second of Eq. (4). The plastic softening (or hardening) frictional behaviour starts when the value of τ exceeds the limit $\tilde{n}$, which is a function of the normal applied stress.

The proposed plastic function was developed to obtain a single yield function for different materials. The adopted plastic function is expressed as follows:

$$H_n(\alpha) = b_1(\alpha_n + b_5)^{b_4} + b_2\alpha_n + b_3 \tag{6}$$

$$H_t(\alpha) = b_1(\alpha_t + b_5)^{b_4} + b_2\alpha_t + b_3 \tag{7}$$

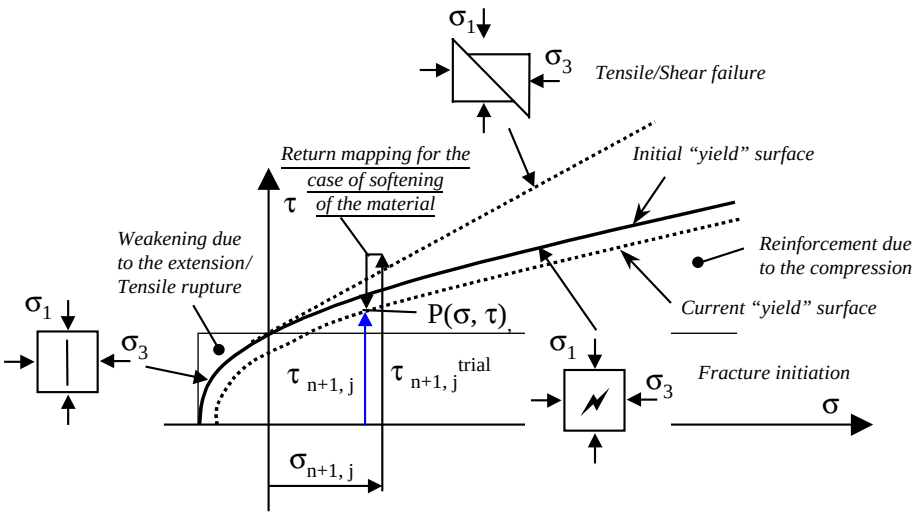

Fig. 3. Schematization of the 2D yield locus for one-dimensional constitutive law.

where b_1, b_2, b_3, b_4 and b_5 are the parameters of plastic function, which are defined separately for normal tension, normal compression and shear actions. By changing these parameters we can define different shapes of the yield surface and consequently simulate very different soil and rock behaviours.

3. Sensitivity analysis of the plastic function

The parameters of the plastic function at microscopic level do not have a real physical meaning. For this reason, as previously stated, we tune them through trial and error procedure: it will be shown that if the microscale behaviour is realistic the behaviour of regular and irregular arrays of spheres can be simulated with a suitable upscaling laws. Another reason to use the trial and error is that we are developing also another procedure, using the ANN, to move from micro- to macromodel (Nardin et al., 2003b).

In order to analyse the influence of the various parameters on the plastic behaviour of the material, the sensitivity of the response of some material parameters is investigated. These parameters are related to the behaviour of the plastic function and the results of these analyses are shown in the sequel.

By analyzing the variation of parameters b_1, b_2, b_3, b_4, and b_5 it is possible to deduce the shape of the softening curve and reproduce the possible real physical behaviour at macrolevel. For constant b_1, b_3, b_4, and b_5 values the plastic surface in function of α_i and b_2 is depicted in Fig. 4. The $|b_2|$ increments increase the residual strength in compression. This means that when b_2 decreases the material becomes more ductile. In Fig. 5 the bi-dimensional elasto-plastic stress–strain relationships for different values of b_2 are collected.

The effect of a $b_1 = |b_3|$ increment in the plastic function, keeping the other parameters constant, is depicted in Fig. 6. A bi-dimensional representation of the global yield curve in Fig. 7 is shown. In these cases when b_1 increases the material presents an increasing brittleness and a decrease of residual strength in compression. Moreover the curvature of the plastic function increases when b_1 decreases (see curve $b_1 = 2.5$ in Fig. 7).

Finally the variation of b_4 is studied, keeping constant the other parameters. On the contrary of the previous cases, when b_4 increases the material presents an increasing ductility and a greater residual strength in compression. As limit case when b_4 is equal to zero the material becomes elastic perfectly plastic (curve $b_4 = 0$ in Fig. 8).

The mutual variation of all parameters determines different softening behaviour of the material. First, when contemporarily b_1 and $|b_3|$ increase and b_4 decreases we obtain a very brittle material: after the peak stress the strength of the material suddenly drops (curve $b_4 = -9000$ in Fig. 8). On contrary, a very ductile

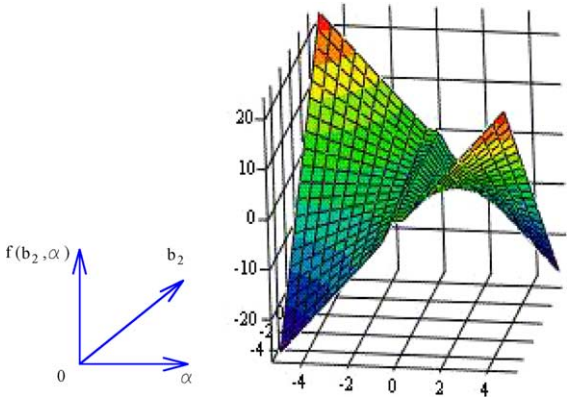

Fig. 4. Three-dimensional representation of the plastic function: variation of the b_2 and α parameter's.

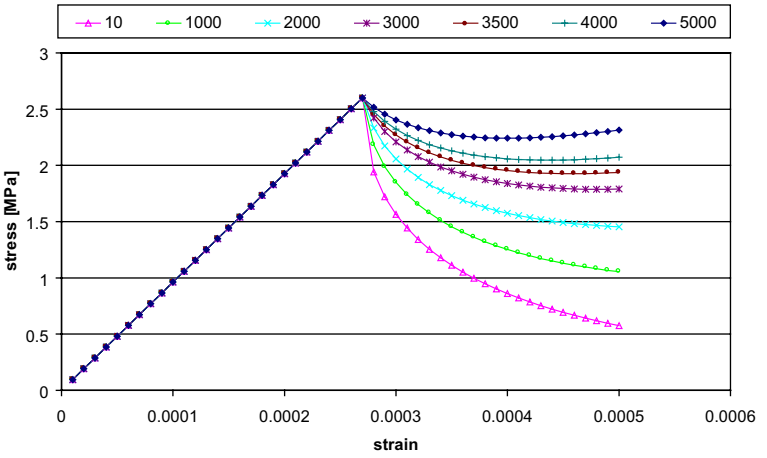

Fig. 5. Stress–strain relationship of an ideal material: numerical results for different values of b_2 (uniaxial test).

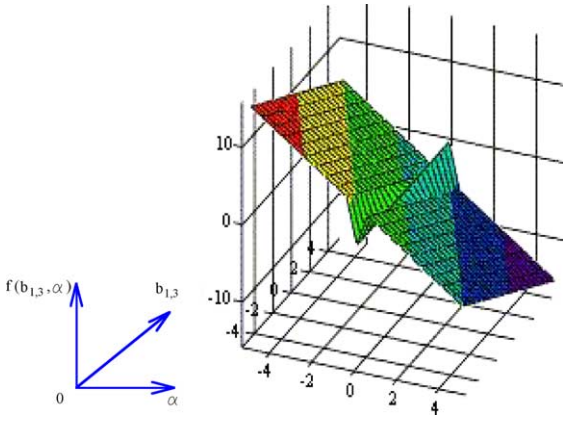

Fig. 6. Three-dimensional representation of the plastic function: variation of the b_1, b_3 and α parameter's.

material can be defined by decreasing b_1 and $|b_3|$ and increasing b_4. All intermediate combinations of parameter values define various softening behaviours.

4. Numerical applications

The numerical simulation of uniaxial traction and compression for different materials is carried out through the micromechanical model, following the experimental procedure proposed by Okubo and Fukui (1996).

We try to obtain qualitatively the real behaviour and define, by trial and error procedure, the values of the microparameters. These parameters, in fact, at microscopic level do not have a real physical meaning. In the next Section we propose some scaling laws to move from the microscopic to the macroscopic level to reproduce the behaviour of a real soil sample.

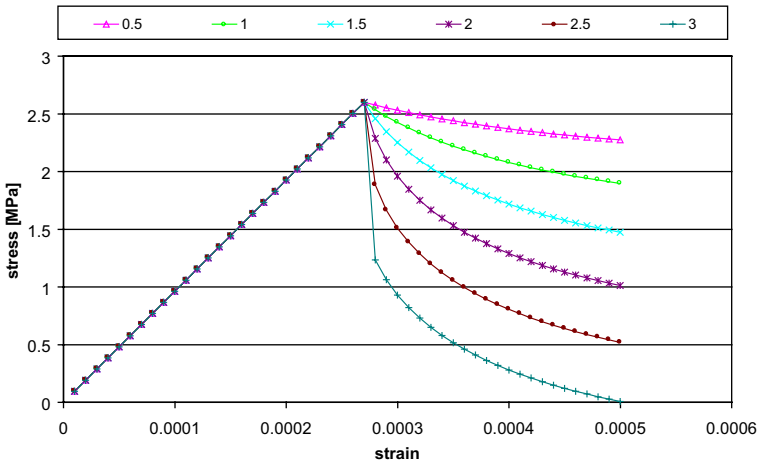

Fig. 7. Stress–strain relationship of an ideal material: numerical results for different values of b_1 and b_3 (uniaxial test).

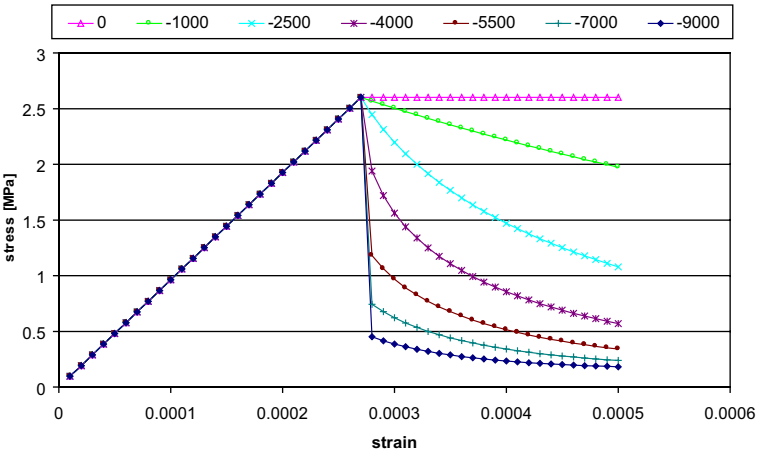

Fig. 8. Stress–strain relationship of an ideal material: numerical results for different values of b_4 (uniaxial test).

4.1. Akiyoshi marble

The plastic function for this material is linear in compression and hyperbolic in tension. The comparison between numerical and experimental results is shown in Figs. 9 and 10. All the values of the tuned parameters are listed in Table 1.

4.2. Kimachi sandstone

As for the previous materials the micromechanical model is tuned by trial and error procedure to approximate as well as possible the real behaviour of this rock. All the parameters are collected in the Table 2.

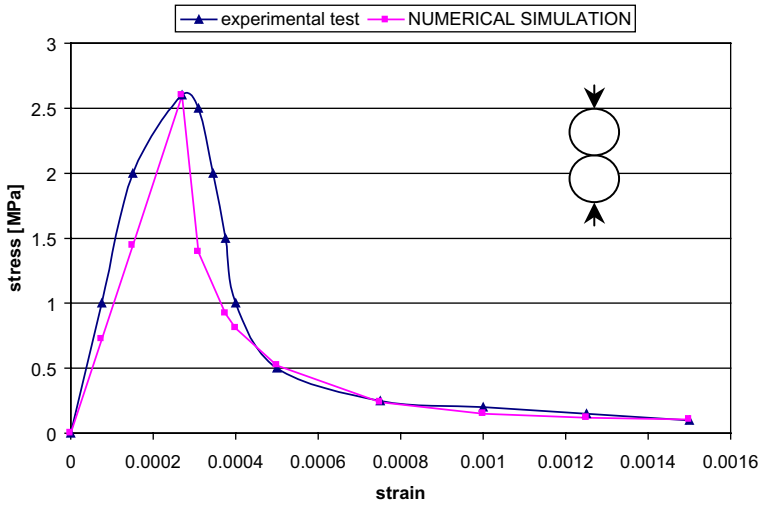

Fig. 9. Uniaxial traction test for Akiyoshi marble: comparison between the experimental test and numerical simulation obtained with the micromechanical model.

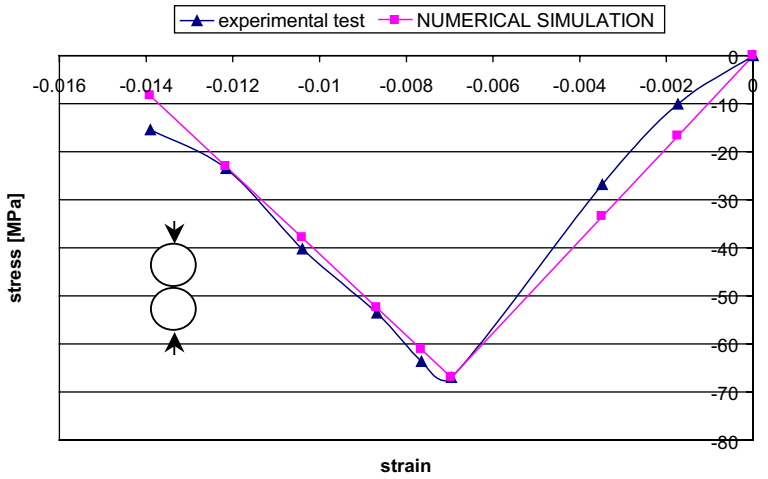

Fig. 10. Uniaxial compression test for Akiyoshi marble: comparison between the experimental test and numerical simulation obtained with the micromechanical model.

The comparison of the results of the numerical model and experimental test are shown in Fig. 11. These results evidence that the new law can capture also the behaviour of quite brittle material as the Kimachi sandstone. Here the plastic function is the algebraic composition of linear and hyperbolic functions.

4.3. Tako sandstone

As previously described, also for Tako sandstone a numerical simulation of the uniaxial traction through the micromechanical model is carried out. The parameters of the contact law, which are tuned by trial and

Table 1
Parameters for normal and tangential contact laws for Akiyoshi marble

Parameters for normal contact law	
$E_n = 9.629E+9$ N/m^2	Young's modulus
$H_n(\alpha) = b_1(\alpha_n + b_5)^{b_4} + b_2\alpha_n + b_3$	Plastic function for normal contact
Parameters for *compression*	
$b_1 = 0.0$, $b_2 = -4.5\times10^3$, $b_3 = 0.0$, $b_4 = 1.0$, $b_5 = 0.0$, $\sigma_c = 67.0E+6$ N/m^2	Yield stress (force) for compression
Parameters for *traction*	
$b_1 = 2.45$, $b_2 = 0.0$, $b_3 = -2.45$, $b_4 = -4.0\times10^3$, $b_5 = 1.0$, $\sigma_t = 2.6E+6$ N/m^2	Yield stress (force) for traction
$g_n = 0.00025$ m	Critical displacement (traction cut-off)
Parameters for tangential contact law	
$E_t = 3.5E+9$ N/m^2	Tangential modulus
$H_t(\alpha) = b_1(\alpha_t + b_5)^{b_4} + b_2\alpha_t + b_3$	Plastic function for shear field
$b_1 = 0.0$, $b_2 = -1.0\times10^3$, $b_3 = 0.0$, $b_4 = 1.0$, $b_5 = 0.0$, $g_t = 0.0058$ mm	Critical displacement value for tangential stress
Yield stress function for tangential contact $n(\sigma_n)$	
$c = 1.0$, $\eta = 0.7$, $n(\sigma_n) = \eta\cdot(c + \sigma_n)$	Limit of elastic field

Table 2
Parameters for normal and tangential contact laws for Kimachi sandstone

Parameters for normal contact law	
$E = 4.9E+9$ N/m^2	Young's modulus
Plastic function	
$H_n(\alpha) = b_1(\alpha_n + b_5)^{b_4} + b_2\alpha_n + b_3$	
Parameters for *traction*	
$b_1 = 2.7$, $b_2 = -4.695\times10^2$, $b_3 = -2.7$, $b_4 = -5.0\times10^3$, $b_5 = 1.0$, $\sigma_t = 3.5E+6$ N/m^2	Yield stress (force) for traction
$g_n = 0.025$ m	Critical displacement (traction cut-off)
Parameters for tangential contact law	
$E_t = 1.8E+9$ N/m^2	Tangential modulus
$H_t(\alpha) = b_1(\alpha_t + b_5)^{b_4} + b_2\alpha_t + b_3$	Plastic function for shear field
$b_1 = 0.0$, $b_2 = -1.0\times10^3$, $b_3 = 0.0$, $b_4 = 1.0$, $b_5 = 0.0$ $g_t = 0.0025$ mm	Critical displacement value for tangential stress
Yield stress function for tangential contact $n(\sigma_n)$	
$c = 1.0$	Cohesive contribute
$\eta = 0.7$	Stress field parameter
$n(\sigma_n) = \eta\cdot(c + \sigma_n)$	Limit of elastic field

error procedure, are summarized in Table 3. In all these cases the behaviour of the chosen plasticity functions seems satisfactory (see also Fig. 12).

5. Macromechanical model

This section deals with the macroscale description of regular packings of disks, starting from microscale parameters, by defining a transition between the micro- and macromechanical models as shown below.

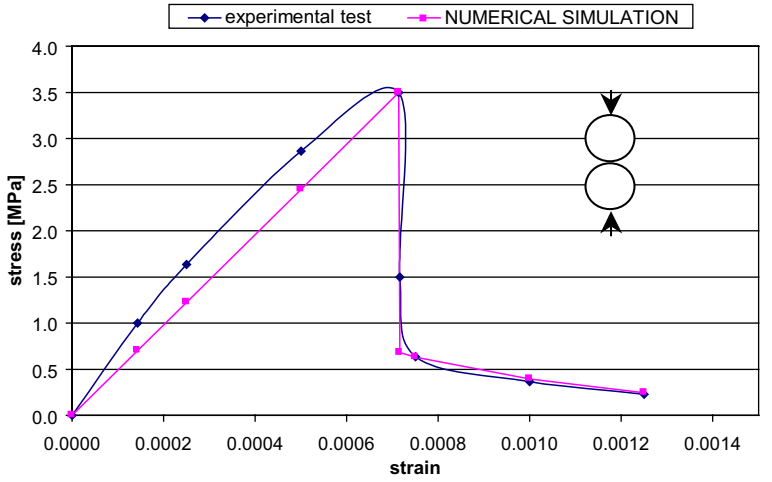

Fig. 11. Uniaxial traction tests for Kimachi sandstone: comparison between the experimental test and numerical simulation obtained with the micromechanical model.

Table 3
Parameters for normal and tangential contact laws for Tako sandstone

Parameters for normal contact law	
$E_n = 4.0E+9$ N/m^2	Young's modulus
Plastic function	
$H_n(\alpha) = b_1(\alpha_n + b_5)^{b_4} + b_2\alpha_n + b_3$	
Parameters for *traction*	
$b_1 = 2.2$, $b_2 = -4.695\times10^3$, $b_3 = -2.2$, $b_4 = -4.5\times10^3$, $b_5 = 1.0$, $\sigma_t = 3.0E+6$ N/m^2	Yield stress (force) for traction
$g_n = 0.025$ mm	Critical displacement (traction cut-off)
Parameters for tangential contact law	
$E_t = 1.8E+9$ N/m^2	Tangential modulus
$H_t(\alpha) = b_1(\alpha_t + b_5)^{b_4} + b_2\alpha_t + b_3$	Plastic function for shear field
$b_1 = 0.0$, $b_2 = 0.0$, $b_3 = 0.0$, $b_4 = 1.0$, $b_5 = 0.0$, $g_t = 0.00125$ mm	Critical displacement value for tangential stress
Yield stress function for tangential contact $n(\sigma_n)$	
$c = 1.0$	Cohesive contribute
$\eta = 0.7$	Stress field parameter
$n(\sigma_n) = \eta \cdot (c + \sigma_n)$	Limit of elastic field

The very complex nature of the problem and the different adopted models show that the influence of the microscale parameters on the strength properties is not uniquely defined (Walton, 1987; Misra and Chang, 1993). The theory of asymptotic homogenization was used in (Huang et al., 1998) with a different contact model. Here we use another procedure for the discrete-continuum linkage: the scaling laws for material properties at the two levels (micro and macro) are constructed using dimensional analysis (Buckingham theorem, Becker, 1976; Kaneko et al., 2003) and numerical uniaxial tests.

Our goal is to carried out a first attempt to define a relation between the micro- and macroparameters by performing several numerical simulation of standard tests, such as uniaxial traction and compression.

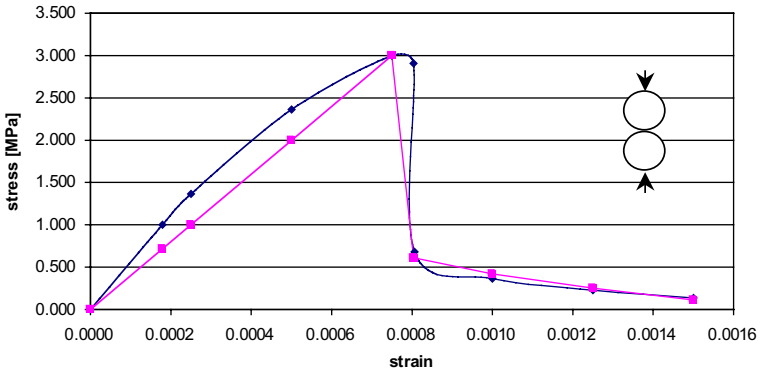

Fig. 12. Uniaxial traction tests for Tako sandstone: comparison between the experimental test and numerical simulation obtained with the micromechanical model.

The obtained numerical results are fitted through a power function which relates some micro- and macro-parameters.

For these reasons a particle assembly with the following characteristic: $H/L \cong 2$, $L/R = 25$, $R_{\mathrm{dev}}/R = 0$, $R = 0.5$ mm is constructed. This represents standard initial configuration and is denoted as "Configuration O". This standard sample contains about 1250 particles. Its porosity with a near zero mean stress is around $n = 22\%$.

The elasto-plastic properties and uniaxial strengths of a particle assembly are examined using the response of this disks assembly of size $L \times H$ under uniaxial compression or tension.

Here we report the final results only, for more specific considerations about this procedure the reader is referred e.g. to Nardin (2003).

The dependence of the elastic constants on the micromechanical parameters is expressed through the following scaling laws:

$$E = E_{\mathrm{n}} \Phi_E \left(\frac{E_{\mathrm{t}}}{E_{\mathrm{n}}}, \frac{L}{R} \right) \tag{8}$$

$$v = \Phi_v \left(\frac{E_{\mathrm{t}}}{E_{\mathrm{n}}}, \frac{L}{R} \right) \tag{9}$$

where v is the real Poisson ratio, the functions Φ_E and Φ_v are dimensionless, R is the disk radius and E (the real Young modulus) can be scaled by either E_{n} or E_{t}. The "real values" refer to the continuum.

Similarly, the compressive strength of the material, Σ_{n}, and the tensile strength, Σ_{t}, can be written as

$$\Sigma_{\mathrm{c}} = S \Phi_{\mathrm{c}} \tag{10}$$

$$\Sigma_{\mathrm{t}} = S \Phi_{\mathrm{t}} \tag{11}$$

where the scaling quantity S can be chosen as one of the following parameters $E_{\mathrm{n}}, E_{\mathrm{t}}, \sigma_{\mathrm{t}}/R, n(\sigma_{\mathrm{n}})/R$. The scale function can be expressed as

$$\Phi_{\mathrm{c,t}} = \Phi_{\mathrm{c,t}} \left(\frac{ER}{\sigma_{\mathrm{n,t}}}, \frac{n(\sigma_{\mathrm{n}})}{\sigma_{\mathrm{n,t}}}, \frac{G}{E}, \frac{L}{R} \right) \tag{12}$$

This last function is defined with respect to the quantity used to scale the strength.

In this way the dependence of the scaled parameters, σ_c/Σ_c and the scaled Young modulus E on the ratio L/R are determined. As previously stated, the numerical curve obtained through the uniaxial tests has been fitted. The fitting function is represented in both cases by an exponential curve (see also Nardin, 2003)

$$y = Ae^{(-Cx)} + B \tag{13}$$

where y and x correspond in the case of Eq. (8) respectively to the scaled Young modulus E and ratio L/R. The values of the parameters A, B and C are: $A=-2.0$, $B=0.98$, $C=0.260$.

The same fitting function is used for Eqs. (10) and (11), but in this case y and x correspond, respectively, to σ_c/Σ_c and the ratio L/R. In this case the values of the parameters A, B and C are: $A=1.4$; $B=0.04$; $C=26.5$.

As previously stated, the plastic microparameters do not have a real physical meaning and do not have corresponding macroparameters. However, we can observe that the plastic function defines the slope of the stress–strain relationship in the plastic range as the elastic modulus defines the slope in the elastic range. For this reason a scaling law similar to Eq. (8) is applied to the parameters of the plastic function.

6. Numerical applications with regular packing (1250 disks)

The uniaxial traction tests of the same specimens of Section 4 are simulated with a regular packing of 1250 disks. The radius of the disks is 0.5 mm. Starting from the parameters defined in Section 4 these values are tuned for the different materials as shown in the sequel.

6.1. Akiyoshi marble

In this simulation the real behaviour of the rock is reproduced (see Figs. 13 and 14). The discrepancies with the experimental results are more evident in the elastic range of the traction test (Fig. 13), while in the compression test the results of the numerical model correspond quite well with the real behaviour of the

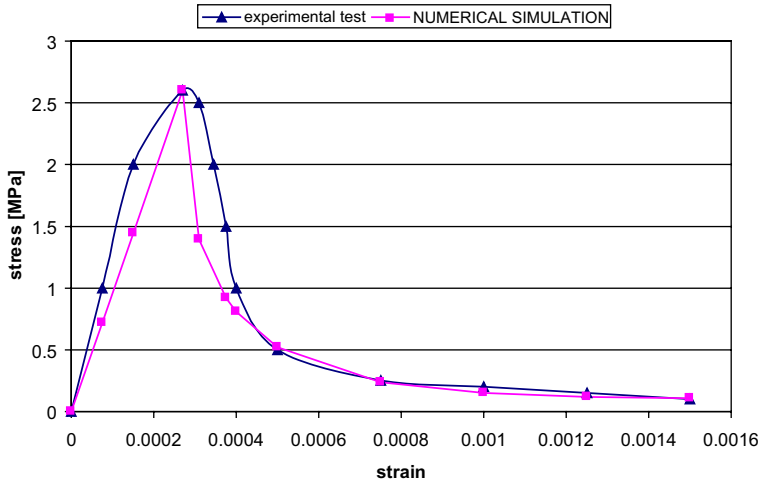

Fig. 13. Uniaxial traction test for Akiyoshi marble: comparison between the experimental test and numerical simulation with a collection of 1250 disks.

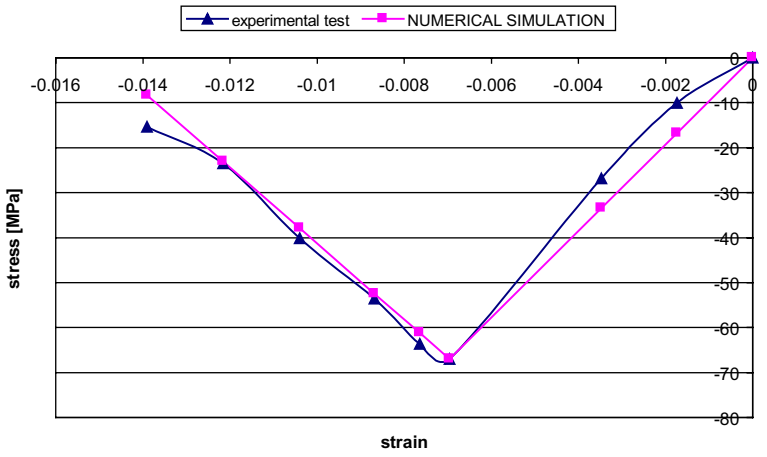

Fig. 14. Uniaxial compression test for Akiyoshi marble: comparison between the experimental test and numerical simulation with a collection of 1250 disks.

Table 4
Contact parameters for Akiyoshi marble: regular packing of 1250 disks

Parameters for normal contact law	
$E_n = 9.243E+9$ N/m^2	Young's modulus
$H_n(\alpha) = b_1(\alpha_n + b_5)^{b_4} + b_2\alpha_n + b_3$	Plastic function for normal direction
Parameters for *compression*	
$b_1 = 0.0$, $b_2 = -4.320\times10^3$, $b_3 = 0.0$, $b_4 = 1.0$, $b_5 = 0.0$, $\sigma_c = 134.0E+6$ N/m^2	Yield stress (force) for compression
Parameters for *traction*	
$b_1 = 4.9$, $b_2 = 0.0$, $b_3 = -4.9$, $b_4 = -2.0\times10^3$, $b_5 = 1.0$, $\sigma_t = 5.2E+6$ N/m^2	Yield stress (force) for traction
$g_n = 0.025$ m	Critical displacement (traction cut-off)
Parameters for tangential contact law	
$E_t = 2.1551E+9$ N/m^2	Tangential modulus
$H_t(\alpha) = b_1(\alpha_t + b_5)^{b_4} + b_2\alpha_t + b_3$	Plastic function for shear field
$b_1 = 0.0$, $b_2 = 1.0\times10^3$, $b_3 = 0.0$, $b_4 = 1.0$, $b_5 = 0.0$, $g_t = 0.00175$ mm	Critical displacement value for tangential stress
Yield stress function for tangential contact $n(\sigma_n)$	
$c = 1.0$	Cohesive contribute
$\eta = 0.7$	Stress field parameter
$n(\sigma_n) = \eta\cdot(c + \sigma_n)$	Limit of elastic field

material (Fig. 14). All the tuned parameters of this material are collected in Table 4. A comparison with Table 1 shows the influence of the scaling procedure.

In the case of a regular array of disks the parameter values obtained with the proposed scaling laws reproduce well the actual behaviour of the different rocks. There is, in fact, a good coincidence between the numerical results of the micro- and macromodels. This is due to the fact that in a regular packing the contact distribution is homogeneous and the number of active contact points for each disks is constant during the tests. This permits to obtain the same results with different number of disks.

6.2. Kimachi sandstone

The studied material is the Kimachi sandstone characterized by

1. density $\vartheta = 2.17$ g/cm^3;
2. modulus of elasticity $E = 4.9E+9$ N/m^2;
3. compressive strength $\sigma_c = 32.0E+6$ N/m^2;
4. tensile strength $\sigma_t = 3.5E+6$ N/m^2.

This material is tested only in uniaxial traction and the test is conducted under displacements control. The experimental stress–strain curve of the uniaxial traction test of the Kimachi sandstone is depicted in Fig. 15. From the analysis of this curve it is possible to underline that Kimachi sandstone is a rock that presents a relatively ductile behaviour. The stress–strain curve in the pre-failure elastic range starts to deviate from the linear behaviour at an early stage and the non-linear elastic behaviour is relatively larger than that of granite and andesite. After the peak load the strength of the material suddenly drops to 20% of the peak value. After this loss of strength the loading capacity decreases continuously until it reaches 5% of the peak strength, as depicted in Fig. 15. The parameters at contact level are tuned and normalized respect to the height of the specimen. The values of these parameters are summarized in Table 5. The comparison between the numerical and experimental results shows that also in this case the model is able to capture the real material behaviour. This is specially true for the softening branch of the stress–strain curve. Again Figs. 15 and 11 are very similar: a good approximation at microscopic level is necessary for this method to obtain a satisfactory behaviour at macroscopic level, which is needed for real simulation.

6.3. Tako sandstone

The studied material is the Tako sandstone rock characterized by the following properties:

1. density $\vartheta = 2.16$ g/cm^3;
2. modulus of elasticity $E = 4.0E+9$ N/m^2;

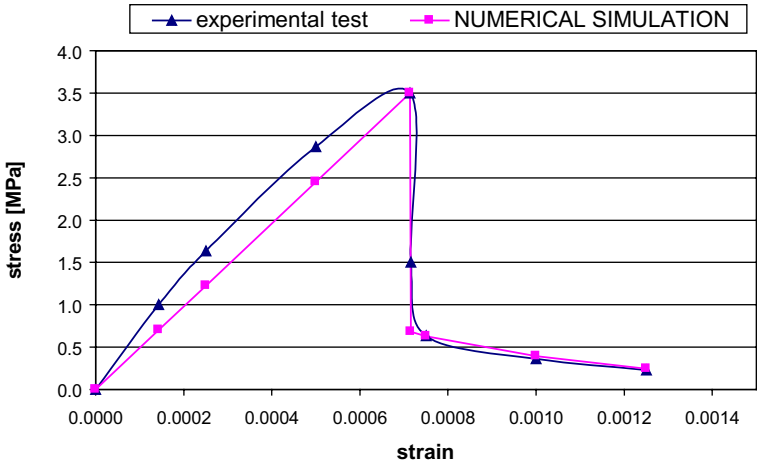

Fig. 15. Uniaxial traction test for Kimachi sandstone: comparison between the experimental test and numerical simulation with a collection of 1250 disks.

Table 5
Contact parameters for Kimachi sandstone: regular packing of 1250 disks

Parameters for normal contact law	
$E_n = 4.820E+9$ N/m^2	Young's modulus
$H_n(\alpha) = b_1(\alpha_n + b_5)^{b_4} + b_2\alpha_n + b_3$	Plastic function for normal direction
Parameters for *traction*	
$b_1 = 5.4$, $b_2 = 0.0$, $b_3 = -5.4$, $b_4 = -2.45\times10^3$, $b_5 = 1.0$, $\sigma_t = 7.0E+6$ N/m^2	Yield stress (force) for traction
$g_n = 0.025$	Critical displacement (traction cut-off)
Parameters for tangential contact law	
$E_t = 1.8E+9$ N/m^2	Tangential modulus
$H_t(\alpha) = b_1(\alpha_t + b_5)^{b_4} + b_2\alpha_t + b_3$	Plastic function for shear field
$b_1 = 0.0$, $b_2 = -2.94\times10^3$, $b_3 = 0.0$, $b_4 = 1.0$, $b_5 = 0.0$, $g_t = 0.0025$ mm	Critical displacement value for tangential stress
Yield stress function for tangential contact $n(\sigma_n)$	
$c = 1.0$	Cohesive contribute
$\eta = 0.7$	Stress field parameter
$n(\sigma_n) = \eta\cdot(c + \sigma_n)$	Limit of elastic field

3. compressive strength $\sigma_c = 32.0E+6$ N/m^2;
4. tensile strength $\sigma_t = 3.0E+6$ N/m^2.

This material is tested only in uniaxial traction and the test is conducted under control of displacements. The experimental stress–strain curve of the uniaxial traction test of the Tako sandstone is depicted in Fig. 16. From this curve it is possible to see that Tako sandstone is also a rock-material that presents a relatively ductile behaviour. The peak stress of the Tako sandstone is considerably smaller than that of Kimachi sandstone. However, the stress–strain curve of the two sandstones presents little difference in the global shape. In fact, also for Tako sandstone the stress–strain curve in the elastic range deviates from the linear behaviour at an early stage.

After the peak load the strength of the material suddenly drops to 23% of the peak value: after this the loading capacity decreases continuously until it reaches 2% of the peak strength, as shown in Fig. 16.

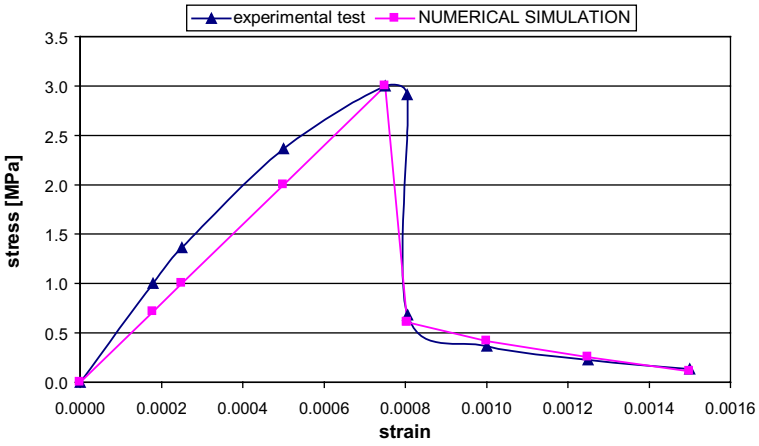

Fig. 16. Uniaxial traction test for Tako sandstone: comparison between the experimental test and numerical simulation with a collection.

Table 6
Contact parameters for Tako sandstone: regular packing of 1250 disks

Parameters for normal contact law	
$E_n = 3.92E+9$ N/m^2	Young's modulus
$H_n(\alpha) = b_1(\alpha_n + b_5)^{b_4} + b_2\alpha_n + b_3$	plastic function for normal direction
Parameters for *traction*	
$b_1 = 4.4$, $b_2 = 0.0$, $b_3 = -4.4$, $b_4 = -2.25\times10^3$, $b_5 = 1.0$, $\sigma_t = 6.0E+6$ N/m^2	Yield stress (force) for traction
$g_n = 0.025$ mm	Critical displacem. (traction cut-off)
Parameters for tangential contact law	
$E_t = 1.764E+9$ N /m^2	Tangential modulus
$H_t(\alpha) = b_1(\alpha_t + b_5)^{b_4} + b_2\alpha_t + b_3$	Plastic function for shear field
$b_1 = 0.0$, $b_2 = 0.0$, $b_3 = 0.0$, $b_4 = 1.0$, $b_5 = 0.0$, $g_t = 0.00125$ mm	Critical displacement value for tangential stress
Yield stress function for tangential contact $n(\sigma_n)$	
$c = 1.0$	Cohesive contribute
$\eta = 0.7$	Stress field parameter
$n(\sigma_n) = \eta \cdot (c + \sigma_n)$	Limit of elastic field

In this simulation the original size of the real specimen is reproduced: the specimen is discretized with a collection of 1250 disks. Also in this case the upscaling procedure to obtain correct value of parameters of micromechanical model is applied. The comparison between experimental results and numerical simulation is depicted in Fig. 16. The values of the parameters at contact level were tuned as shown in Table 6.

7. Numerical applications with irregular packing (1250 disks)

So far only the macroscale material properties of "Configuration O" have been studied. In order to investigate the dispersion of material properties of an irregular assembly due to the random generating algorithm, five different configurations have been generated with the same geometrical parameters as "Configuration O". The contact properties for these configurations are taken to be the same as those of Section 5.

The uniaxial traction tests of the same specimens of Section 4 are simulated with an irregular packing of 1250 disks. The radius of the disks is 0.5 mm.

The irregular packing of the disks is obtained by imposing a random geometrical perturbation on the initial geometrical arrangement. This was obtained by a variation of the coordinates of several disks in the initial configuration (see Fig. 17), as shown in Borja and Wren (1995).

The analysis of several numerical tests evidenced that:

- to obtain the same uniaxial strength and Young modulus (in traction and compression) with the irregular packing it is necessary change the value of the normal and tangential contact stiffness in a range of ≅20%, respect the regular packing;
- this variation is due to the different number of active contacts in function of random packing (this is in good accordance with (Chang and Misra, 1990; Bathurst and Rothenburg, 1992)).

On the basis of these considerations, starting from the parameters defined in Section 4, the values of the microparameters are tuned using the relations (8)–(13) for the different materials as shown in the sequel.

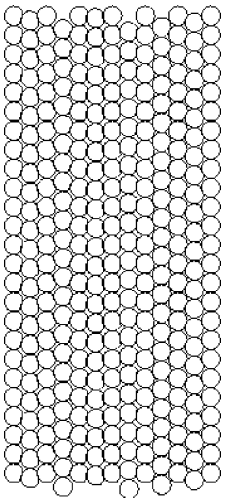

Fig. 17. Example of irregular packing of disks.

7.1. Akiyoshi marble

In this simulation the real behaviour of the rock is reproduced (see Fig. 18). The discrepancies with the micromechanical model are more evident in the plastic range of the traction test (Fig. 18), while the elastic part corresponds quite well with the behaviour of the micromechanical model. All the tuned parameters of this material are collected in Table 7. A comparison with Table 4 shows the influence of the scaling procedure.

The values of the microparameters, determined with the scaling laws, capture the macrobehaviour of the irregular packing under uniaxial traction. It is possible to remark that only the normal contact stiffness is changed respect with the regular packing. This is due, as previously stated, to the global increment of active contacts. The new values of the contact stiffnesses are determined through numerical tests. The comparison between the results of the regular and irregular packing shows that in the irregular one the influence of the tangential component and of the increasing number of contact points produce a more brittle behaviour.

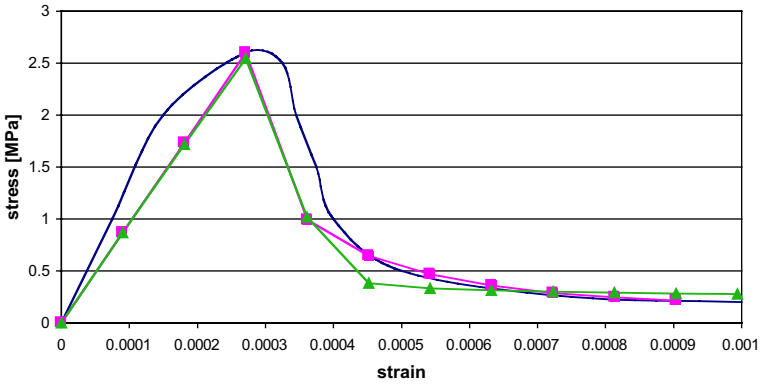

Fig. 18. Uniaxial traction test for Akiyoshi marble: comparison between the experimental test and numerical micro- and irregular macromodel.

Table 7
Contact parameters for Akiyoshi marble: irregular packing of 1250 disks

Parameters for normal contact law	
$E_n = 7.450E+9$ N/m^2	Young's modulus
$H_n(\alpha) = b_1(\alpha_n + b_5)^{b_4} + b_2\alpha_n + b_3$	Plastic function for normal direction
Parameters for *compression*	
$b_1 = 0.0$, $b_2 = -4.320\times10^3$, $b_3 = 0.0$, $b_4 = 1.0$, $b_5 = 0.0$, $\sigma_c = 134.0E+6$ N/m^2	Yield stress (force) for compression
Parameters for *traction*	
$b_1 = 4.9$, $b_2 = 0.0$, $b_3 = -4.9$, $b_4 = -2.0\times10^3$, $b_5 = 1.0$, $\sigma_t = 5.2E+6$ N/m^2	Yield stress (force) for traction
$g_n = 0.025$ m	Critical displacement (traction cut-off)
Parameters for tangential contact law	
$E_t = 2.1551E+9$ N/m^2	Tangential modulus
$H_t(\alpha) = b_1(\alpha_t + b_5)^{b_4} + b_2\alpha_t + b_3$	Plastic function for shear field
$b_1 = 0.0$, $b_2 = 1.0\times10^3$, $b_3 = 0.0$, $b_4 = 1.0$, $b_5 = 0.0$, $g_t = 0.00175$ mm	Critical displacement value for tangential stress
Yield stress function for tangential contact $n(\sigma_n)$	
$c = 1.0$	Cohesive contribute
$\eta = 0.7$	Stress field parameter
$n(\sigma_n) = \eta\cdot(c + \sigma_n)$	Limit of elastic field

7.2. Tako sandstone

The numerical simulation of the Tako sandstone is carried out using the same random packing of disks of the Akiyoshi marble. The comparison between experimental results and numerical simulation is depicted in Fig. 19. The values of the parameters at contact level are tuned as shown in Table 8.

In this case the reproduction of the "brittle" softening behaviour of this material presents some drawbacks. In fact, there are discrepancies with the micromechanical model especially in the plastic range. The residual tensile stress is almost 20% larger with respect to the real behaviour of the material. A possible explanation of this difference is that the Tako sandstone presents a very brittle behaviour: in this case the tuning of the cut-off tensile value influences contemporarily the peak stress and the residual tensile stress. Also in this case the comparison between the regular and irregular packings shows that the irregular array

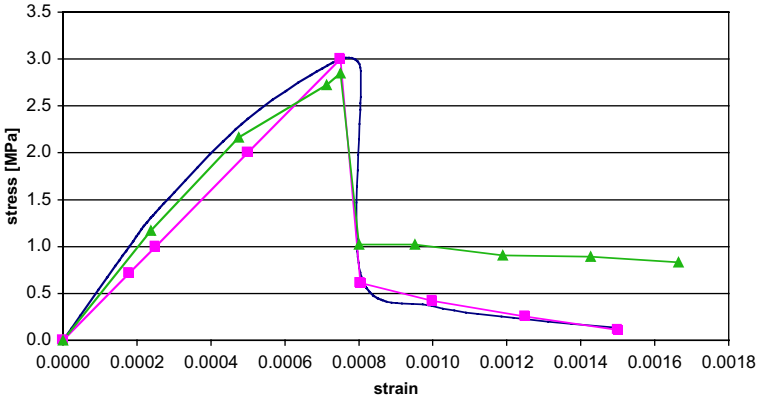

Fig. 19. Uniaxial traction test for Tako sandstone: comparison between the experimental test and numerical micro- and irregular macromodel.

Table 8
Contact parameters for Tako sandstone: irregular packing of 1250 disks

Parameters for normal contact law	
$E_n = 3.270E+9$ N/m^2	Young's modulus
$H_n(\alpha) = b_1(\alpha_n + b_5)^{b_4} + b_2\alpha_n + b_3$	Plastic function for normal direction
Parameters for *traction*	
$b_1 = 4.4$, $b_2 = 0.0$, $b_3 = -4.4$, $b_4 = -2.25\times10^3$, $b_5 = 1.0$, $\sigma_t = 6.0E+6$ N/m^2	Yield stress (force) for traction
$g_n = 0.025$ mm	Critical displacement (traction cut-off)
Parameters for tangential contact law	
$E_t = 1.8E+9$ N/m^2	Tangential modulus
$H_t(\alpha) = b_1(\alpha_t + b_5)^{b_4} + b_2\alpha_t + b_3$	Plastic function for shear field
$b_1 = 0.0$, $b_2 = 0.0$, $b_3 = 0.0$, $b_4 = 1.0$, $b_5 = 0.0$, $g_t = 0.00125$ mm	Critical displacement value for tangential stress
Yield stress function for tangential contact $n(\sigma_n)$	
$c = 1.0$	Cohesive contribute
$\eta = 0.7$	Stress field parameter
$n(\sigma_n) = \eta \cdot (c + \sigma_n)$	Limit of elastic field

presents a more brittle behaviour. Otherwise, the elastic part corresponds quite well with the micromechanical model. The comparison shown in Fig. 19 evidences, however, that the shape of the curves of the micro- and macromodels is similar.

8. Conclusions

A quasi-static model based on a collection of disks in contact has been enhanced by adopting sophisticated contact models. With these models we have simulated the experimentally observed soil behaviour. In the first part we concentrate our attention on the contact formulation and on the constitutive model for normal and tangential contact. We have shown that with a simple model, composed of two disks in contact, real constitutive behaviour can be obtained. We have also carried out a sensitivity analysis on the parameters of the local contact laws. In the second part we have focused our attention on a collection of disks and on parameters tuning. With a regular and irregular packing of more than 1000 disks we have simulated the real behaviour of soils and rocks. Finally we have compared the results of the micro- and macromechanical models.

Acknowledgments

Financial support of EU (project GRD1-1999-10330 "CUTTER") and of MURST (ex 60%) "Sviluppo di modelli meccanici e costitutivi termodinamicamente coerenti per i mezzi porosi multiphase" is gratefully acknowledged. We wish to thank also Prof. Giorgio Zavarise and all the collaborators of the "CUTTER" project.

References

Bathurst, R., Rothenburg, L., 1992. Investigation of micromechanical features of idealized granular assemblies using DEM. Eng. Computat. 9, 199–210.

Becker, H.A., 1976. Dimensionless Parameters: Theory and Methodology. John Wiley and Sons, New Year.
Borja, R., Wren, J.R., 1995. Micromechanics of granular media. Part I: Generation of overall constitutive equation fro assemblies of circular disks. Comput. Meth. Appl. Mech. Engrg. 127, 13–36.
Chang, C., Misra, A., 1990. Packing structure and mechanical properties of granulates. J. Eng. Mech. 116 (5), 1077–1093.
Cundall, P.A., Strack, D.L., 1979. A discrete numerical model for granular assemblies. Géotechnique 29, 47–65.
Emeriault, F., Cambou, B., 1996. Micromechanical modeling of anisotropic non-linear elasticity of granular medium. Int. J. Solids Struct. 33 (18), 2591–2607.
Huang, H., Damjanac, B., Detournay, E., 1998. Normal wedge indentation in rocks with lateral confinement. Rock Mech. Rock Eng. 31 (2).
Kaneko, K., Terada, K., Kyoya, T., Kishino, Y., 2003. Global–local analysis of granular media in quasi-static equilibrium. Int. J. Solids Struct. 40 (15), 4043–4069.
Lefik, M., Schrefler, B.A., 2002. Artificial neural network for parameter identifications for an elasto-plastic model of superconducting cable under cyclic loading. Comput. Struct. 80 (22), 1699–1713.
Misra, A., Chang, C.S., 1993. Effective elastic moduli of heterogeneous granular solids. Int. J. Solids Struct. 30 (18), 2547–2566.
Nardin, A., 2003. Discrete methods for soil modelling. Ph.D. Thesis. Department of Structural and Transportations Engineering, University of Padua, Italy.
Nardin, A., Zavarise, G., Schrefler, B.A., 2003a. Modelling of cutting tool–soil interaction—part I: contact behaviourComputational Mechanics, vol. 31. Springer-Verlag, Berlin, pp. 327–339.
Nardin, A., Schrefler, B.A., Lefik, M., 2003b. Application of artificial neural network for identification of parameters of a constitutive law for soilsLecture Notes in Artificial Intelligence (LNAI), vol 2718. Springer-Verlag, Heidelberg, pp. 545–554.
Okubo, S., Fukui, K., 1996. Complete stress–strain curves for various rock types in uniaxial tension. Int. J. Rock Mech. Miner. Sci. Geomech. Abstr. 33 (6), 549–556.
Potyondy, D., Cundall, P., Lee, C., 1996. Modelling rock using bonded assemblies of circular particles. In: Aubertin, M., Hassani, F., Mitri, H. (Eds.), Proceedings of the 2nd NARMS, Rock Mechanics Tools and Techniques. Balkema, Montreal, pp. 1937–1944.
Simo, J.C., Hughes, T.J., 1998. Computational Inelasticity: Computational Aspects. Springer-Verlag, Telos.
Walton, K., 1987. The effective elastic moduli of a random packing of spheres. J. Mech. Phys. Solids 35 (2), 213–226.
Zavarise, G., Wriggers, P., Stein, E., Schrefler, B., 1992. Real contact mechanism and finite element formulation- a coupled thermomechanical approach. Int. J. Numer. Methods Eng. 35, 767–785.